Full Wave Analyses of Electromagnetic Fields With an Iterative Domain Decomposition Method

Amane Takei[1], Shin-Ichiro Sugimoto[1], Masao Ogino[2], Shinobu Yoshimura[1], and Hiroshi Kanayama[2]

[1]Department of Systems Innovation, School of Engineering, The University of Tokyo, Tokyo 113-8656, Japan
[2]Department of Mechanical Engineering, Faculty of Engineering, Kyushu University, Fukuoka 819-0395, Japan

This paper describes large-scale full wave analyses of electromagnetic fields by the finite-element method with an iterative domain decomposition method (IDDM). A stationary vector wave equation for the high-frequency electromagnetic field analyses is solved taking an electric field as an unknown function. Then, to solve subdomain problems by the direct method, the direct method based on the LDL^T decomposition method is introduced in subdomains. If the direct method is applied for solving subdomain problems, the computation time seems to be reduced by the improved accuracy of subdomain problems, and storing matrices that are results of the decomposition on main memory.

***Index Terms*—Finite-element method (FEM), hierarchical domain decomposition method (HDDM), high-frequency electromagnetic field, vector wave equations.**

I. Introduction

THE finite-element method (FEM) has been used to solve the vector wave equations in high-frequency electromagnetic problems, resulting in solving large-scale systems of simultaneous linear equations. Dealing with such large-scale problems is a crucial issue in solving system of equations derived from the finite-element discretization of the vector wave equations in high-frequency electromagnetic problems [1]. Currently, we are conducting research on large-scale finite-element analyses for electromagnetic fields in the range of several megahertz to several gigahertz by using parallelization techniques based on the iterative domain decomposition method (IDDM). For the high-frequency electromagnetic problems, the conjugate orthogonal conjugate gradient (COCG) method is applied to solve the interface problem of the IDDM. Previously, an iterative method was applied to subdomain problems. However, the convergence property of the interface problem was not good in solving large-scale problems of over ten million complex degrees of freedom (DOFs). To improve this issue, the direct method based on the LDL^T decomposition method is applied to subdomain problems. In this paper, we provide numerical examples of about 100 million complex DOFs based on the formulation of the E-method [2]. To the best of our knowledge, there has currently been no publication about large-scale high-frequency problems with several hundred million complex DOFs using unstructural meshes [3], [4].

II. Finite-Element Formulation

A. Vector Wave Equations

Let Ω be a domain with the boundary $\partial\Omega$. The vector wave equations which describe an electromagnetic field with single angular frequency ω [rad/s] are drawn from Maxwell's equations containing the displacement current. The vector wave equations describing an electric field $\mathbf{E}$ [V/m] are given by (1a) and (1b), using the current density $\mathbf{J}$ [A/m ^{2}] and the electric field $\mathbf{E}$, and assigning j as an imaginary unit

$$\mathrm{rot}(1/\mu \mathrm{rot}\mathbf{E}) - \omega^2\varepsilon\mathbf{E} = j\omega\mathbf{J}, \quad \text{in } \Omega \tag{1a}$$

$$\mathbf{E}\times\mathbf{n} = \mathbf{0}, \quad \text{on } \partial\Omega \tag{1b}$$

$$\mathbf{J} = \sigma\hat{\mathbf{E}}. \tag{1c}$$

Permittivity and permeability are given by ε [F/m] and μ [H/m], respectively. In this formulation, the permittivity becomes complex permittivity $\varepsilon = \varepsilon' + \sigma/j$. The electric field $\hat{\mathbf{E}}$ on known points is substituted into (1a) by (1c), where the electrical conductivity is denoted as σ. By solving (1a), with imposing the boundary condition of (1b), we calculate the electric field $\mathbf{E}$. The magnetic field $\mathbf{H}$ is then calculated from the electric field $\mathbf{E}$ by postprocessing using (2), which is one of Maxwell's equations [2] as follows:

$$\mathrm{rot}\,\mathbf{E} - j\omega\mu\mathbf{H} = \mathbf{0}. \tag{2}$$

B. E-Method

Next, we describe the finite-element discretization. The electric field $\mathbf{E}$ is approximated with Nedelec elements (edge elements) [5], [6]. The finite-element approximation is performed as follows.

Find $\mathbf{E}_h$ such that

$$(1/\mu\mathrm{rot}\mathbf{E_h}, \mathrm{rot}\mathbf{E_h^*}) - \omega^2(\varepsilon\mathbf{E_h}, \mathbf{E_h^*}) = j\omega(\mathbf{J_h}, \mathbf{E_h^*}) \tag{3}$$

where $(\cdot,\cdot)$ denotes the complex valued L^2-inner product. Here, $\mathbf{J_h}$ is an electric current density approximated by the conventional piecewise linear tetrahedral elements.

III. Iterative Domain Decomposition Method

A. Interface Problem

We introduce the IDDM to high-frequency problems using the E-method. Let us put the finite-element equations of (3) in matrix form, as follows:

$$Ku = f \tag{4}$$

Manuscript received December 23, 2009; accepted February 15, 2010. Current version published July 21, 2010. Corresponding author: A. Takei (e-mail: takei@save.sys.t.u-tokyo.ac.jp).

Digital Object Identifier 10.1109/TMAG.2010.2044775

where K denotes the coefficient matrix, u is the unknown vector, and f is the known right-hand side vector. As shown in the following equation, the domain Ω is decomposed into N pieces so that there is no overlap in the boundary between subdomains, namely

$$\Omega = \bigcup_{i=1}^{N} \Omega^{(i)}. \tag{5}$$

After domain decomposition, (4) is rewritten as follows:

$$\begin{bmatrix} K_{II}^{(1)} & \cdots & 0 & K_{IB}^{(1)} R_B^{(1)^T} \\ \vdots & \ddots & \vdots & \vdots \\ 0 & \cdots & K_{II}^{(N)} & K_{IB^{(N)}} R_B^{(N)^T} \\ R_B^{(1)} K_{IB}^{(1)^T} & \cdots & R_B^{(N)} K_{IB}^{(N)^T} & \sum_{i=1}^{N} R_B^{(i)} K_{BB}^{(i)} R_B^{(i)^T} \end{bmatrix} \times \begin{bmatrix} u_I^{(1)} \\ \vdots \\ u_I^{(N)} \\ u_B \end{bmatrix} = \begin{bmatrix} f_I^{(1)} \\ \vdots \\ f_I^{(N)} \\ \sum_{i=1}^{N} R_B^{(i)} f_B^{(i)} \end{bmatrix} \tag{6}$$

where subscripts I, B correspond to nodal points in the interior of subdomains, on the interface boundary, respectively. Here, $R_B^{(i)^T}$ relates the internal DOFs $u_B^{(i)}$ of subdomain $\Omega^{(i)}$ with u_B. It is a 0-1 procession to restrict. Equations (7) and (8) are obtained from (6)

$$K_{II}^{(i)} u_I^{(i)} = f_I^{(i)} - K_{IB}^{(i)} u_B^{(i)}, \qquad i = 1, \ldots, N \tag{7}$$

$$\left\{ \sum_{i=1}^{N} R_B^{(i)} \left\{ K_{BB}^{(i)} - K_{IB}^{(i)^T} \left(K_{II}^{(i)} \right)^{-1} K_{IB}^{(i)} \right\} R_B^{(i)^T} \right\} u_B = \sum_{i=1}^{N} R_B^{(i)} \left\{ f_B^{(i)} - K_{IB}^{(i)^T} \left(K_{II}^{(i)} \right)^{-1} f_I^{(i)} \right\} \tag{8}$$

where $\sum R_B^{(i)} f_B^{(i)} (i = 1, \ldots, N)$ is the right-hand side vector of the equation regarding u_B. Equation (8) represents the interface problem of enforcing the continuity between subdomains in the domain decomposition method. Here, $(K_{II}^{(i)})^{-1}$ is the inverse matrix of $K_{II}^{(i)}$. Next, (8) is rewritten as

$$S u_B = g \tag{9}$$

where S is described as follows:

$$S = \sum_{i=1}^{N} R_B^{(i)} S^{(i)} R_B^{(i)^T} \tag{10}$$

$$S^{(i)} = K_{BB}^{(i)} - K_{IB}^{(i)^T} \left(K_{II}^{(i)} \right)^{-1} K_{IB}^{(i)}. \tag{11}$$

Here, S and $S^{(i)}$ are the Schur complement matrix and the local Schur complement matrix in subdomain $\Omega^{(i)}$, respectively.

B. Computing Procedure

As shown in Fig. 1, the algorithm based on the COCG method is applied to solve the interface problem shown in (9), and the internal boundary DOF u_B is calculated first. Here, δ is a nonnegative constant used for testing convergence, and $\| \cdot \|$ indicates the Euclidean norm. Because the construction of the Schur complement matrix S requires a very large amount of computation time, we replace it with substeps (a) and (b), which are executed in each COCG step. Although a dot product operation must be performed for both substeps, the overall computation time is greatly reduced. Finally, the solution of a whole domain

Choose u_B^0

$p^0 = r^0 = S u_B^0 - g$ ····· (a)

for $n = 0,1,.....$

$q^n = S p^n$ ····· (b)

$\alpha^n = \dfrac{(r^n)^T r^n}{(p^n)^T q^n}$

$u_B^{n+1} = u_B^n - \alpha^n p^n$

$r^{n+1} = r^n - \alpha^n q^n$

IF $\left\| r^{n+1} \right\| < \delta \left\| r^0 \right\|$, break

$\beta^n = \dfrac{(r^{n+1})^T r^{n+1}}{(r^n)^T r^n}$

$p^{n+1} = r^{n+1} + \beta^n p^n$

end

(a) In each subdomain

Compute $u_I^{(i)0}$ by

$$K_{II}^{(i)} u_I^{(i)0} = f_I^{(i)} - K_{IB}^{(i)} R_B^{(i)^T} u_B^0$$

$$r^{(i)0} = K_{IB}^{(i)^T} u_I^{(i)0} + K_{BB}^{(i)} R_B^{(i)^T} u_B^0 - f_B^{(i)}$$

$$p^0 = r^0 = \sum_{i=1}^{N} R_B^{(i)} r^{(i)0}$$

(b) In each subdomain

Compute $p_I^{(i)n}$ by

$$K_{II}^{(i)} p_I^{(i)n} = -K_{IB}^{(i)} R_B^{(i)^T} p^n$$

$$q^{(i)n} = K_{IB}^{(i)^T} p_I^{(i)n} + K_{BB}^{(i)} R_B^{(i)^T} p^n$$

$$q^n = \sum_{i=1}^{N} R_B^{(i)} q^{(i)n}$$

Fig. 1. Algorithm based on the COCG method in the interface problem.

can be obtained by calculating each subdomain DOF $u_I^{(i)}$ from (7). The finite-element computations of (a), (b), and (7) can be performed by the direct method with the LDL^T decomposition method on each subdomain independently.

IV. Hierarchical Domain Decomposition Method

The original analysis domain is first divided into parts, which are further decomposed into smaller domains called subdomains. This is called the hierarchical domain decomposition method (HDDM) [7].

In the hierarchical processor mode (H-mode) [8], processors are classified into three groups: grandparent, parent, and child. One of the processors is assigned as grandparent, a few as parent, and others as child. The number of parent processors is the same as that of the parts. The number of child processors can be varied; and it affects parallel performance. However, because most communication time is spent between parent processors and child processors, the communication speed is important. Although computer performance has been improved by advances in network technology in recent years, a high-speed network is still expensive. Generally in PC clusters often used, network speed is a bottleneck degrading the

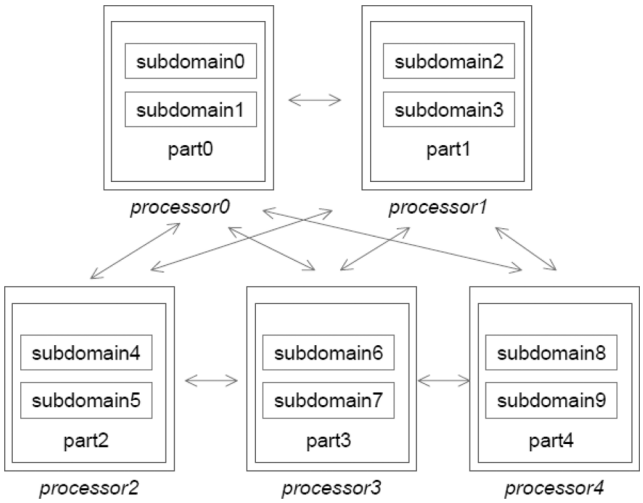

Fig. 2. Data distribution and communication in the parallel processor mode.

processing performance of the CPU. Moreover, when parallel processing performance is considered, it is important to reduce an amount of communications as much as possible. Therefore, the parent-only type [parallel processor mode (P-mode)] is more useful than the H-mode that uses all three groups [2], [9].

In the P-mode, only parent processors perform the finite-element analysis (FEA), which in the H-mode is computed by child processors. In the H-mode, although parent processors store some of the subdomain analysis data and coordinate the COCG iterations as primary work, the idle time of the CPU increases because the parent processors perform fewer computations. In contrast, in P-mode, all processors in the P-mode perform the FEA, and every CPU can be used without idleness in an environment with 10–20 CPUs. Thus, the P-mode is considered superior to the H-mode in an aspect of performance. In the P-mode, the number of parent processors should be equal to that of the parts (Fig. 2).

V. Numerical Examples

A. Whole Body Cavity Resonator

A reentrant-type cavity resonator model is used to verify the accuracy and performance of the parallel computation of our proposed method. The cavity has a diameter of 1.90 m and a height of 1.45 m. In this analysis, the dielectric phantom of the shape of a disk with specific dielectric constant $\varepsilon_r = 80$ and electric conductivity $\sigma = 0.52$ S/m is placed, and the resonance state is investigated. This problem is one of the benchmark problems defined as Testing Electromagnetic Analysis Method (TEAM) Workshop Problem 29 [10]. The analysis model is shown in Fig. 3(a). The mesh, divided into first-order tetrahedral Nedelec elements, is shown in Fig. 3(b).

Verifications are performed on five kinds of meshes, described in Table I. Meshes (i)–(v) are divided into first-order tetrahedral Nedelec elements. As in our previous work involving high-frequency problems [2], the highest computation efficiency is achieved when the number of elements contained in one subdomain is about 170, and the number of subdomains

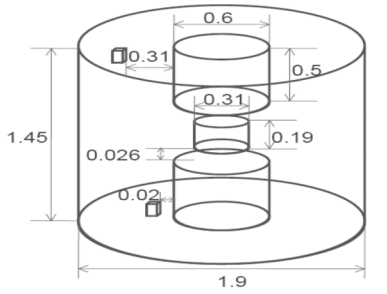

(a)

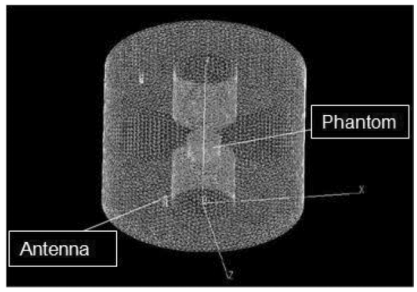

(b)

Fig. 3. TEAM Workshop Problem 29. (a) Sketch of the model (unit: meter). (b) Mesh.

TABLE I
Meshes for Verifications

Mesh	Num. of elements	DOF	Num. of subdomains
(i)	108,787	134,889	640
(ii)	5,043,711	6,792,202	29,680
(iii)	17,367,244	23,213,252	98,160
(iv)	40,349,688	54,236,667	239,760
(v)	95,811,411	111,871,716	658,000

is determined as such as that the number of elements contained in one subdomain is equal to 170.

B. Accuracy Verification

Accuracy verification is performed using mesh (i). To detect the resonant frequency and to compare solutions with actual measurements, the resonance state is investigated. The frequency band of 60–200 MHz is calculated for 2- and 0.4-MHz steps around resonant frequencies, and the response for every frequency step is investigated. All computations are performed on a 20-node (80-core) PC cluster with Intel Core i7 940 (2.93 GHz/L2 256 KB/L3 8 MB/Quad Core/QPI 4.8 GTs) and 12-GB RAM. The frequency response of the magnetic field is shown in Fig. 4.

A comparison between the measured resonant frequencies [10] and the solutions obtained by the finite-difference time-domain (FDTD) method [10] in each mode is shown in Table II. This comparison method is the same as in [10]. The obtained solutions are in very good agreement. The maximum error rate between the obtained solution and the measurement is 4.96% in the first mode. As the mode becomes higher, the error rate decreases. It is thought that this tendency is natural, because the same tendency is shown in the comparison of the error rate with solution of the FDTD method. Therefore, it is proved that the solution obtained by the proposed method has sufficiently high accuracy.

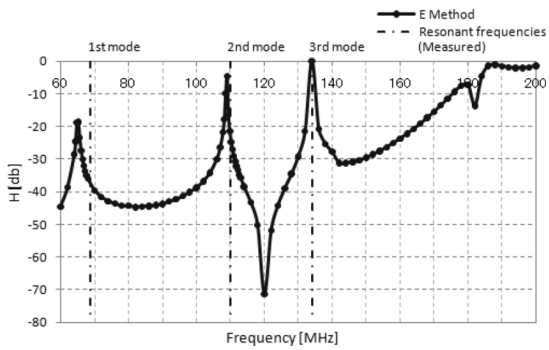

Fig. 4. Comparison of frequency responses with measured data. [Mesh (i)].

TABLE II
RESONANT FREQUENCIES IN MEGAHERTZ [(): ERROR RATE BETWEEN MEASURED DATA AND NUMERICAL SOLUTIONS (IN PERCENT)]

Mode	Measured	FDTD 25mm mesh	Result
1st	68.6	67 (2.33)	65.2 (4.96)
2nd	110	110	109 (0.91)
3rd	134	134	134

TABLE III
CPU TIME AND MEMORY REQUIREMENTS FOR EACH MESH

Mesh	Solver for subdomains	Iteration counts	CPU time[h]	Memory size [MB]
(ii)	LDL^T	5,926	0.6	64
	ICCOCG	12,046	2.1	44
(iii)	LDL^T	9,411	2.1	217
	ICCOCG	—	—	—
(iv)	LDL^T	17,437	7.8	551
	ICCOCG	—	—	—
(v)	LDL^T	23,393	20.4	1,210
	ICCOCG	—	—	—

C. Performance Verification

Performance verification by large-scale computation using meshes (ii)–(v) is described next. In the analyses, the first mode (65.2 MHz) frequency is analyzed. Other computation conditions are the same as those for mesh (i). CPU time and average memory per core are shown in Table III.

For mesh (ii) in solving with the direct method based on the LDL^T decomposition method to subdomain problems, the CPU time is reduced by 71% as compared to that of the COCG method with the incomplete Cholesky factorization (ICCOCG) to subdomain problems. For meshes (iii)–(v), solving with the ICCOCG method to subdomain problems does not converge, but the direct method successfully converges to compute a result. Although the direct method uses approximately 45% more memory, the total amount used exceeds 40% of the available RAM even for mesh (v). Therefore, we do not consider memory usage to be a problem. The residual norm convergence history of COCG iterations in the interface problem is shown in Fig. 5. In the computations with mesh (v), we can see the history of the residual norm in the interface problem in the case of the ICCOCG method to subdomain problems. Here the interface problem does not converge even after 40 000 iterations. In contrast, by the direct method, convergence is achieved after 23 393 iterations with a computation time of 20.4 h. Those results confirm the superiority of the direct method to subdomain problems in large-scale computations. It is also demonstrated that the proposed method using the direct method for subdomain problems is able to solve high-frequency electromagnetic field problems with more than 100 million complex DOFs.

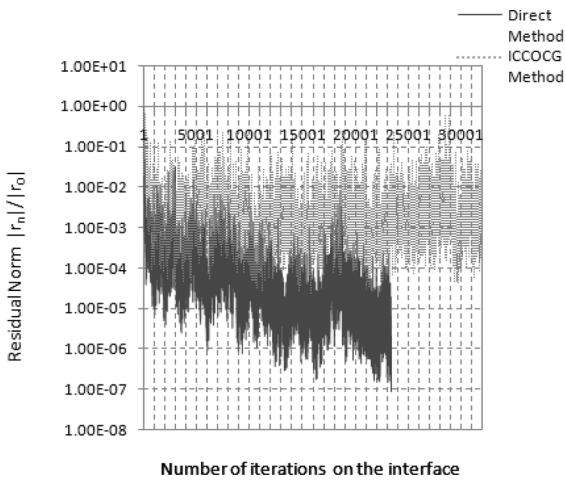

Fig. 5. Histories of residual norms on the interface. [Mesh (v)].

VI. CONCLUSION

To improve the convergence in the interface problem of the IDDM, we have introduced the direct method based on the LDL^T decomposition method in subdomains. As a result, we have confirmed improvement of the convergence in the interface problem. Moreover, we have shown the possibility of solving high-frequency problems with 100 million complex DOFs. In future researches, it is very important for us to reduce number of iterations and computational time by devising algorithms.

REFERENCES

[1] P. Liu and Y. Q. Jin, "The finite-element method with domain decomposition for electromagnetic bistatic scattering from the comprehensive model of a ship on and a target above a large-scale rough sea surface," *IEEE Trans. Geosci. Remote Sens.*, vol. 42, no. 5, pp. 950–956, 2004.

[2] A. Takei, S. Yoshimura, and H. Kanayama, "Large-scale parallel finite element analyses of high frequency electromagnetic field in commuter trains," *CMES*, vol. 31, no. 1, pp. 13–24, 2009.

[3] Y. J. Li and J. M. Jin, "Implementation of the second-order ABC in the FETI-DPEM method for 3D EM problems," *IEEE Trans. Antennas Propag.*, vol. 56, no. 8, pp. 2765–2769, Aug. 2008.

[4] T. Ha, S. Seo, and D. Sheen, "Parallel iterative procedures for a computational electromagnetic modeling based on a nonconforming mixed finite element method," *CMES*, vol. 14, no. 1, pp. 57–76, 2009.

[5] F. Kikuchi, "Numerical analysis of electrostatic and magnetostatic problems," *Sugaku Expositions*, vol. 6, no. 1, pp. 33–51, 1993.

[6] H. Kanayama and S. Sugimoto, "Effectiveness of A-ϕ method in a parallel computing with an iterative domain decomposition method," *IEEE Trans. Magn.*, vol. 42, no. 4, pp. 539–542, Apr. 2006.

[7] S. Yoshimura, R. Shioya, H. Noguchi, and T. Miyamura, "Advanced general-purpose computational mechanics system for large scale analysis and design," *J. Comput. Math.*, vol. 149, pp. 279–296, 2002.

[8] R. Shioya and G. Yagawa, "Iterative domain decomposition FEM with preconditioning technique for large scale problem," *Proc. Progr. Exp. Comput. Mech. Eng. Mater. Behavior*, pp. 255–260, 1999.

[9] R. Shioya, H. Kanayama, A. M. M. Mukaddes, and M. Ogino, "Heat conductive analysis with balancing domain decomposition method," *J. Theory Mech.*, vol. 52, pp. 43–53, 2003.

[10] Y. Kanai, "Description of TEAM workshop problem 29: Whole body cavity resonator," in *Proc. TEAM Workshop*, Tucson, AZ, 1998.